AIP Advances

RESEARCH ARTICLE | FEBRUARY 05 2024

# Acoustic metamaterials for realizing a scalable multiple phi-bit unitary transformation

K. Runge ; P. A. Deymier ; M. A. Hasan ; T. D. Lata ; J. A. Levine



*AIP Advances* 14, 025010 (2024)
https://doi.org/10.1063/5.0188462

AIP Advances ARTICLE pubs.aip.org/aip/adv

# Acoustic metamaterials for realizing a scalable multiple phi-bit unitary transformation

Cite as: AIP Advances 14, 025010 (2024); doi: 10.1063/5.0188462
Submitted: 4 January 2024 • Accepted: 9 January 2024 •
Published Online: 5 February 2024

View Online Export Citation CrossMark

K. Runge,[1,a),b)] P. A. Deymier,[1,a)] M. A. Hasan,[2,a)] T. D. Lata,[1] and J. A. Levine[3,a)]

## AFFILIATIONS

[1] Department of Materials Science and Engineering, University of Arizona, Tucson, Arizona 85721, USA
[2] Department of Mechanical Engineering, Wayne State University, Detroit, Michigan 48202, USA
[3] Department of Computer Science, The University of Arizona, Tucson, Arizona 85721, USA

[a)] New Frontiers of Sound Science and Technology Center, The University of Arizona, Tucson, AZ 85721, USA.
[b)] **Author to whom correspondence should be addressed:** krunge@arizona.edu

## ABSTRACT

The analogy between acoustic modes in nonlinear metamaterials and quantum computing platforms constituted of correlated two-level systems opens new frontiers in information science. We use an inductive procedure to demonstrate scalable initialization of and scalable unitary transformations on superpositions of states of multiple correlated logical phi-bits, classical nonlinear acoustic analog of qubits. A multiple phi-bit state representation as a complex vector in a high-dimensional, exponentially scaling Hilbert space is shown to correspond with the state of logical phi-bits represented in a low-dimensional linearly scaling physical space of an externally driven acoustic metamaterial. Manipulation of the phi-bits in the physical space enables the implementation of a non-trivial multiple phi-bit unitary transformation that scales exponentially. This scalable transformation operates in parallel on the components of the multiple phi-bit complex state vector, requiring only a single physical action on the metamaterial. This work demonstrates that acoustic metamaterials offer a viable path toward achieving massively parallel information processing capabilities that can challenge current quantum computing paradigms.





## I. INTRODUCTION

Quantum information processing paradigms promise a new era in computational power. A digital quantum computer, constituted of quantum bits (qubits), leverages the properties of the quantum wave function, i.e., a probability amplitude, which can support coherent superpositions of multiple qubit states (e.g., entangled states). However, current quantum computing with multiple qubits suffers from the fragility of quantum superpositions against perturbations (i.e., decoherence) requiring solutions such as cryogenics and error corrections, which use significant hardware and software resources. Quantum computing is essentially phase computing; it exploits the possibility of realizing and rotating the coherent superpositions of states with complex amplitudes of correlated multipartite systems that are represented as vectors in large, exponentially complex Hilbert spaces. Recently, we demonstrated analogies between superpositions of states of acoustic waves and quantum waves, thus potentially offering a decoherence-free acoustic-phase-based computing alternative to quantum systems for some quantum information processing applications.[1–9] The development of an acoustic-based classical quantum-inspired information processing platform necessitates that acoustic waves and their supporting medium satisfy DiVincenzo's five criteria for the physical construction of a quantum computer,[10] which are as follows: "(1) *a scalable physical system with well-characterized qubit;* (2) *the ability to initialize the state of the qubits to a simple fiducial state;* (3) *long relevant decoherence times;* (4) *a 'universal' set of quantum gates;* (5) *a qubit-specific measurement capability.*" In this paper, we briefly review the concept of a logical phase bit (phi-bit),[4] a classical acoustic analog of a qubit, and how superpositions of states of logical phi-bits in externally driven metamaterials satisfy DiVincenzo's criteria.

The notion of acoustic phi-bit originated in the Dirac factorization of the Klein–Gordon-like wave equation for an infinitely long acoustic waveguide coupled to a rigid substrate. This factorization revealed an unconventional wave function: a plane wave whose amplitude is a spinor with complex components. The spinor exposes the two-state nature of the directional degree of freedom (DOF) for propagation along the waveguide in the form of quasi-standing waves with coherent superpositions of forward (F) and backward (B) propagating states.[11] However, stress-free boundary conditions in physical finite length waveguides require that each F and B quasi-standing wave become a full standing wave, thus limiting the detectability of the pseudospin superposition of state.[1] For this reason, we introduced another realization of physical phi-bits in metamaterials constituted of parallel arrays of coupled acoustic waveguides[1,12] The solution of the linear acoustic wave equation separates into the product of two functions, each dependent on DOFs along (wave number) and across the array (e.g., orbital angular momentum[1] or spatial mode[13]). Externally driven resonant spatial modes possess different wave numbers and lead to coherent superpositions of spatial and plane wave product states. The spatial DOF and the plane wave each act as a phi-bit. The state of the coherent superposition can be represented using the usual ket notation of quantum mechanics in the form of $A|E_1\rangle|k_1\rangle + D|E_2\rangle|k_2\rangle$, where $|E_i\rangle$ refer to states associated with the spatial DOF and $|k_j\rangle$ refer to plane wave states. The coefficients $A$ and $D$ are complex resonant amplitudes taking the form of Lorentzian in the presence of dissipative metamaterials. This non-separable superposition is analogous to the non-separable Bell states of quantum mechanics. We experimentally demonstrated that by tuning $A$ and $D$ through the amplitude, phase, and/or frequency of the external drivers, we could experimentally navigate a portion of that acoustic Bell state's Hilbert space[2] to achieve near-maximal classical entanglement as quantified by the "entropy of entanglement," i.e., von Neumann entropy.[2] To explore the complete Hilbert space of product acoustic states—that is, the general superposition, $A|E_1\rangle|k_1\rangle + B|E_1\rangle|k_2\rangle + C|E_2\rangle|k_1\rangle + D|E_2\rangle|k_2\rangle$—we considered an externally driven system composed of a parallel array of 1D waveguides coupled periodically along their length.[14] Band folding within a finite Brillouin zone, due to periodicity, then offers the possibility of selecting spatial and Bloch wave states independently and, thus, the realization of the desired general superposition.

The Hilbert space of a driven two-level spatial DOF $H_1$ is two-dimensional (2D). The Hilbert space of the plane wave states $H_2$ is also 2D, representing the DOF along the waveguides labeled by a two-level wave number with plane wave or Bloch wave basis functions. The Hilbert space tensor product $H = H_1 \otimes H_2$ of these two 2D Hilbert spaces is $2^2$-dimensional. In the case of a periodic system, if we introduce a unit cell with two distinct sites,[14] then we can increase the dimensionality of the product Hilbert space to $2^3$ dimensions. However, to truly exploit the superpositions of acoustic waves in large exponentially complex Hilbert spaces and realize their full potential for quantum information science, it is necessary to elucidate the properties of externally driven arrays of nonlinearly coupled elastic waveguides.[15–17] For instance, in Ref. 17, we theoretically considered the case of $N$ waveguides in a planar array with nonlinear coupling taking the form of a power function of the relative displacements between waveguides with exponent Q. We showed that we can produce a multipartite system composed of two-level phi-bits, which can support coherent superpositions of nonlinear plane wave modes spanning exponentially complex Hilbert spaces of dimension $2^Q$. However, from a practical point of view, this approach is cumbersome due to the need to measure the mixed wave numbers of the nonlinear acoustic plane waves via spatial Fourier transforms.

For this reason, we recently expanded the notion of phi-bits from the physical to the logical realm.[4] For an externally driven array of three coupled acoustic waveguides, we experimentally demonstrated non-separability for the acoustic logical phi-bits that resulted from partitioning in the spectral domain of a nonlinear acoustic field. External drivers nonlinearly mixed the acoustic modes with different frequencies. Subsequently, each logical phi-bit was shown to be a two-level nonlinear mode of vibration whose state is characterized by a nonlinear frequency and spatial mode associated with two independent relative phases between the waveguides. A multipartite composite system composed of $P$ logical phi-bits is then given a representation with a tensor product structure. This representation lies in a $2^P$ dimensional Hilbert space and was shown to support non-separable states for systems with $P$ phi-bits ranging from 3 to 16. This approach offers access to large, scalable, exponentially complex Hilbert spaces supporting non-separable acoustic states.

The ultimate goal of quantum computing is to realize large-scale multiple-qubit unitary operations.[18] However, because of the fragility of quantum superpositions of a large number of qubits, this task is achieved by using the decomposition of large-scale unitary matrices into quantum circuits involving sequences of single- and two-qubit gates[19–23] (DiVincenzo's criterion 4). The challenge is then to determine the minimal quantum circuit that can realize the desired large-scale operation. The primary focus of this work is to show that multiple phi-bit systems can be employed to produce large-scale unitary operations that do not need to be decomposed into circuits of smaller phi-bit gates. Building upon our previous work,[8] which established a correspondence for three correlated logical phi-bits, we extend our analysis to scalable systems encompassing multiple phi-bits. Here, we demonstrate the scalability of multi-phi-bit systems (criterion 1), the ability to initialize multiple phi-bits in some desired state (criterion 2), and the possibility of achieving non-trivial scalable quantum-like gates that go beyond criterion 4. This study represents one more significant step toward the goal of bridging the gap between classical wave science and quantum information science using nonlinear acoustic metamaterials.

## II. LOGICAL PHASE BITS (PHI-BITS) AS QUBIT ANALOGUES

A phi-bit, a classical acoustic analog of a qubit, is a two-state degree of freedom of an acoustic wave, which can be in a coherent superposition of states with complex amplitude coefficients.[24] A logical phi-bit[4] is a two-state degree of freedom in the spectral domain of nonlinear acoustic modes supported by an externally driven array of nonlinearly coupled waveguides (Fig. 1). As nonlinear acoustic modes, logical phi-bits live within the same physical system. They occupy the same real estate—the phi-bit physical system does not need to scale physically. For instance, by using separate waveform generators to excite different waveguides with sinusoidal signals at different frequencies $f_1$ and $f_2$, the displacement field measured at the waveguide's detection ends is the Fourier sum of modes with the

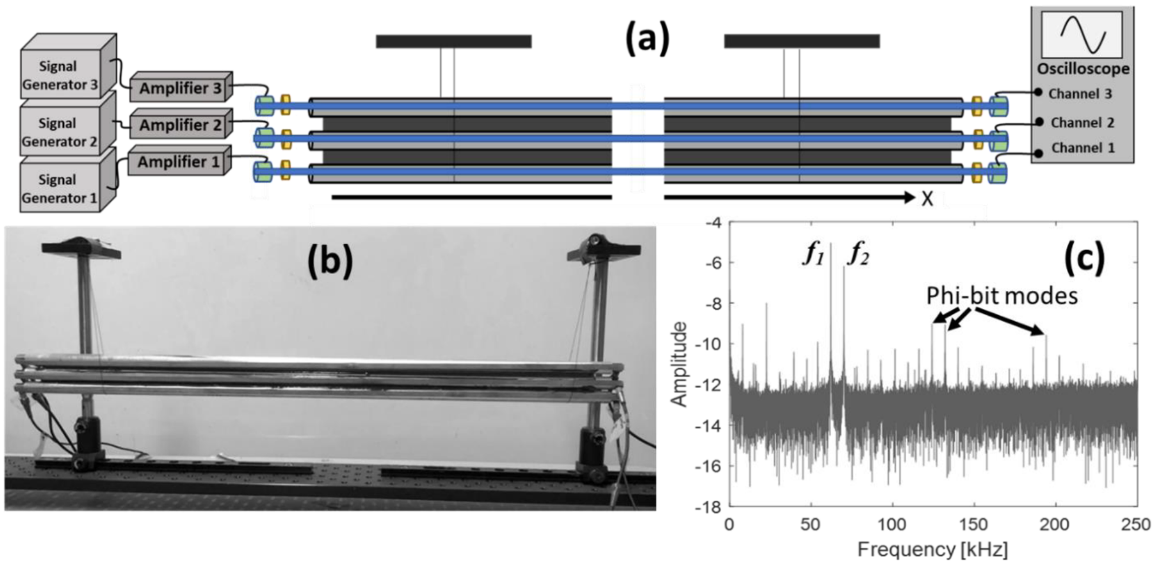


**FIG. 1.** (a) Exploded view and (b) picture of a metamaterial composed of an array of three acoustic waveguides (aluminum rods) coupled with epoxy resin and schematic illustration of the experimental system for generating and detecting logical phi-bits. Three separate signal generators and amplifiers are used to drive piezoelectric transducers. Driving and detecting transducers are attached to the opposite ends of the rod-like acoustic waveguides by the pressure of three independent rubber bands. A thin layer of honey is used as an ultrasonic coupling agent between the transducers and the rod ends. The signals generated by the detecting transducers enter an oscilloscope via independent input channels for analysis. The array of waveguides is suspended by thin threads for isolation. (c) Fourier frequency spectrum calculated from velocity time series measured using a scanning laser Doppler vibrometer. The first and third waveguides are driven at the frequencies $f_1 = 62$ kHz and $f_2 = 66$ kHz, respectively. Examples of nonlinear acoustic modes corresponding to logical phi-bits are indicated as "phi-bit modes" [5,9].

primary frequencies $f_1$ and $f_2$, as well as secondary nonlinear modes whose frequencies are a linear combination of the driving frequencies, $pf_1 + qf_2$, where $p$ and $q$ are integers. Since the logical phi-bits are acoustic modes in the spectral domain with a bandwidth of a few tens of Hz, there is a lot of room in the ultrasonic domain for increasing the number of logical phi-bits beyond the number 50, which is considered to be the threshold for quantum advantage. The displacement field of one logical phi-bit at the end of the three waveguides can be referred to and renormalized to that of the bottom waveguide, 1, in the array to obtain a $2 \times 1$ vector,

$$\boldsymbol{u}^{(p,q)} = \begin{pmatrix} \hat{c}_2 \exp(i\varphi_{12}) \\ \hat{c}_3 \exp(i\varphi_{13}) \end{pmatrix} \exp(i(p\omega_1 + q\omega_2)t), \tag{1}$$

where $\omega_i = 2\pi f_i$; $i = 1, 2$, and the phase difference between the displacement field at waveguides 2 and 3 relative to waveguide 1 are $\varphi_{12} = \varphi_2 - \varphi_1$ and $\varphi_{13} = \varphi_3 - \varphi_1$, respectively. As logical phi-bits are referenced by their values of $p$ and $q$, our physical system supports multiple logical phi-bits each with its own phase differences. The phases $\varphi_1$, $\varphi_2$, and $\varphi_3$ arise from the complex nature of the resonant amplitudes of the driven system with dissipation as well as any nonlinear effect combining these resonant amplitudes. $\hat{c}_2$ and $\hat{c}_3$ are the magnitudes of the acoustic field at the ends of the waveguides 2 and 3, respectively, normalized to the magnitude at the end of waveguide 1. Refer to Fig. 1(a) for the numbering of the waveguides with the external drivers.

We redefine the state of the logical phi-bit $\{p, q\}$, $S_{\boldsymbol{u}^{(p,q)}}$, in terms of phase differences of the displacement field only, by constructing the nontemporal part of the field as the normalized complex amplitude state vector,

$$\left|S_{\boldsymbol{u}^{(p,q)}}\right\rangle = \frac{1}{\sqrt{2}} \begin{pmatrix} \exp(i\varphi_{12}) \\ \exp(i\varphi_{13}) \end{pmatrix} = \frac{1}{\sqrt{2}} (\exp(i\varphi_{12})|0\rangle + \exp(i\varphi_{13})|1\rangle). \tag{2}$$

This state vectors lives on the Bloch sphere, i.e., in the single logical phi-bit 2D Hilbert space, $h$, with basis $\left\{|0\rangle = \begin{pmatrix} 1 \\ 0 \end{pmatrix}, |1\rangle = \begin{pmatrix} 0 \\ 1 \end{pmatrix}\right\}$. The state of each logical phi-bit (i.e., nonlinear mode) is correlated with all other logical phi-bits through the nonlinearity of the system. This enables us to define the state of multiple logical phi-bits as a tensor product of single logical phi-bit states (DiVincenzo's criterion 1). In other words, an $N$ state is defined in an exponentially scaling $2^N$ dimensional Hilbert space, $H$, which is the tensor product of the $N$ Hilbert spaces of the individual logical phi-bits, $H = h_{(1)} \otimes \cdots \otimes h_{(N)}$. A coherent superposition of states of multiple phi-bits can be expressed on the basis vectors, $\langle 00\ldots0|, |00\ldots1\rangle, \ldots, |11\ldots1\rangle$. For example, the $N$ phi-bit state can be written as a tensor product of single phi-bit states,

$$\boldsymbol{V} = \boldsymbol{S}_{(1)} \otimes \boldsymbol{S}_{(2)} \otimes \boldsymbol{S}_{(3)} \ldots \otimes \boldsymbol{S}_{(N)}. \tag{3}$$

Here, we have simplified the notation of Eq. (2) and expressed the state vector $\left|S_{\boldsymbol{u}^{(p,q)}}\right\rangle$ of logical phi-bit "$i$" with $\{p, q\}$ as $\boldsymbol{S}_{(i)}$. The $2^N$

components of a $N$ phi-bit coherent superposition of states are correlated. In other words, a change in the conditions of the physical systems such as in one of the driving frequencies changes all $2^N$ components of the superposition instantaneously.[4] The correspondence between the state of correlated logical phi-bits represented in a low-dimensional linearly scaling physical space of the supporting metamaterial through the pairs of $\varphi_{12}^{(i)}$, $\varphi_{13}^{(i)}$ and the complexity of their state representation in a high-dimensional, exponentially scaling Hilbert space enable the creation of any multiple phi-bit states. By manipulating the physical phi-bit variables and measuring them in the physical space of the system with at most $2 \times N$ dimensions, and by choosing a pertinent representation, one can initialize any coherent superposition of states in the $2^N$-dimensional Hilbert space.[5,9] Coherent superpositions of phi-bit states are acoustic complex amplitudes. These states are not subjected to decoherence, in contrast to the probability amplitude of quantum systems composed of qubits (DiVincenzo's criterion 3).

Measurements in conventional quantum computing approaches entail the collapse of the wavefunction. This is the destruction of the coherent superposition of states that is at the heart of the exponential scaling that leads to quantum advantage. In contrast, measurements in phi-bit systems do not alter the wave function, which persists as long as the drivers are applied (DiVincenzo's criterion 5). Regarding measurement, we note that contact measurement methods become integral parts of the phi-bit supporting physical system. Other methods, such as laser Doppler vibrometry, enable non-contact measurements.[3]

## III. INITIALIZATION AND SCALABILITY OF QUANTUM-LIKE GATES USING PHI-BITS

### A. Background

Quantum computing harnesses the quantum phenomenon of entanglement (i.e., non-separability of superpositions of states). Indeed, even though the Schrödinger equation is linear for a non-interacting multipartite quantum system, Born's rule renders the probability of observations nonlinear functions of the probability amplitude wave function. This phenomenon provides the quantum correlation between the subsystems and the capability of processing in a massively parallel manner information encoded in the multipartite wavefunction. Logical phi-bits are correlated via the nonlinearity of the elasticity of the physical system, while classical entanglement is needed to access regions of Hilbert space with non-separable multi-phi-bit superpositions of states. Acoustic wave entanglement increases the number of possible states and, therefore, the range of information that can be encoded and subsequently processed in those states. Several physical parameters, e.g., frequency, relative phase, or magnitude of the driving forces, can be used to control the coherent superposition of states of the logical phi-bits in their exponentially scaling Hilbert space. By varying a few of these parameters, one operates predictably via unitary operations on the superpositions in the high-dimensional Hilbert space. Unitary operations, mathematically described as unitary transformation matrices, $\boldsymbol{T}$, acting on logical phi-bit state vectors representation, $\boldsymbol{V}$, expressed in some basis, $\{\zeta_1, \zeta_2, \zeta_3, \ldots\}$, that produce the new state vector $\boldsymbol{V}'$ are analogous to quantum gates. A single phi-bit gate operates on states expressed in a 2D basis. A two phi-bit gate operates on the superposition of states expressed on a $2^2 = 4$-dimensional basis, tensor product of the individual phi-bit bases. An $N$ phi-bit gate operates on states supported by an exponentially scaling basis of dimension $2^N$ (Fig. 2). Similar to quantum computers, it is this exponential scaling that potentially gives the advantage of phi-bit-based computing over conventional computing. However, quantum computing faces the challenge of physically operating simultaneously on many qubit states and of maintaining the quantum correlation between qubits during these operations. Strongly nonlinearly correlated logical phi-bits do not suffer from this fragility.

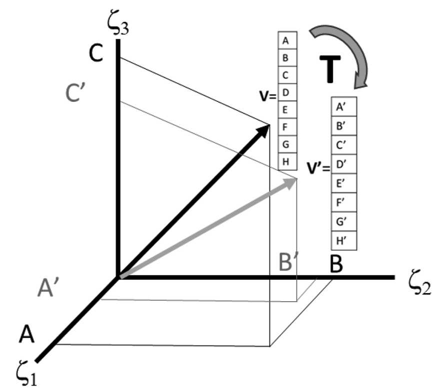


**FIG. 2.** Schematic illustration of quantum-like gate described as a unitary transformation matrix, $\boldsymbol{T}$, acting on an input data string of complex numbers initialized in a multiple logical phi-bit state vector representation, $\boldsymbol{V}$, producing an output data string in the new state vector $\boldsymbol{V}'$. $\{\zeta_1, \zeta_2, \zeta_3, \ldots\}$ is the basis for the representation of $\boldsymbol{V}$ and $V'$.

In that context, we experimentally demonstrated the single phi-bit quantum-like phase and Hadamard gates,[6] and the two phi-bit C-NOT gate.[7] These gates form the components of a universal set of gates (DiVincenzo's criterion 4) that can be used to generate multiple phi-bit quantum-like circuits. However, the power of phi-bit-based computing resides in the scalability of multiple logical phi-bit representations and the robust nonlinear correlation between phi-bits. This allows us to consider the development of large-scale ($N \geq 3$) phi-bit gates that do not need to be decomposed into circuits of small-scale gates and that would, therefore, present challenges for current quantum computing platforms. This development is illustrated in Sec. III B.

### B. Initialization and scalable multi-phi-bit quantum-like gate

We have shown that phi-bit phases $\varphi_{12}$ and $\varphi_{13}$ exhibit a rich set of behaviors resulting from the nonlinearities of the physical system as driving physical parameters such as frequency[5] or phase[9] are varied. These behaviors include, for example, sharp $\pi$ jumps superposed on smooth monotonous background variations (Fig. 3). For all logical phi-bits, the background phases show variations as a function of frequency of several thousand Hz or as a function of drivers' phase, $\Delta\theta$, of tens of degrees. The $\pi$ jumps occur over much shorter frequency intervals of at most a few hundred Hz or a

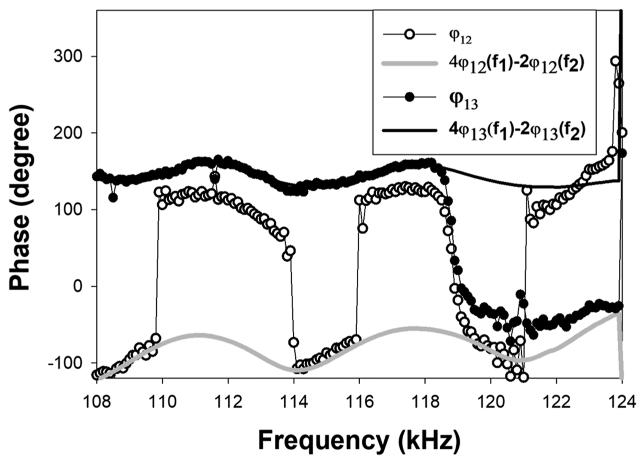


**FIG. 3.** Experimentally measured phases, $\varphi_{12}$ and $\varphi_{13}$, for a phi-bit nonlinear mode with $\{p = 4, q = -2\}$ as a function of its nonlinear frequency $4f_1 - 2f_2$ when the constant frequency $f_1 = 62$ kHz is applied to the first waveguide and the second driving frequency, applied to the third waveguide, is varied in the interval [70–62 kHz] by decreasing increments of 50 Hz. The solid black and gray lines are background phases.

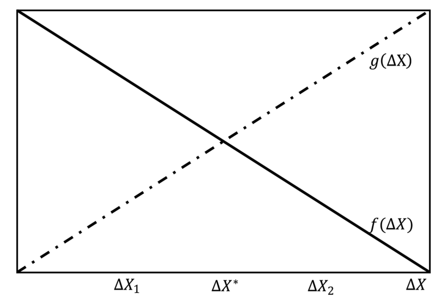


**FIG. 4.** Schematic representation of phi-bit adjusted background phase differences as functions of a change in the driving conditions, $\Delta X$. At $\Delta X^*$, one has $f = g$. $\Delta X_1$ and $\Delta X_2$ are values corresponding to a swap of the values of $f$ and $g$.

few degrees. The background behavior of the phases $\varphi_{12}$ and $\varphi_{13}$ of any logical phi-bit, $pf_1 + qf_2$, can be expressed as the linear combination $p\varphi_{12}(f_1, \Delta\theta) + q\varphi_{12}(f_2, \Delta\theta)$ and $p\varphi_{13}(f_1, \Delta\theta) + q\varphi_{13}(f_2, \Delta\theta)$. In other words, the phases of all logical phi-bit possess a common background behavior that can be related to the phases of the primary modes at the frequencies $f_1$ and $f_2$ with a drivers' phase $\Delta\theta$.

By adding a general phase, one can create regions of driver parameters where the phi-bit background phases $\varphi_{12}$ and $\varphi_{13}$, reduced to the phases of the primary modes, cross and can be exchanged (Fig. 4). We denote these as adjusted background phases. Therefore, phi-bits have relatively adjusted phases that vary in the same way upon tuning one of the physical parameters. In that case, $\varphi_{12}^{(1)} = \varphi_{12}^{(2)} = \varphi_{12}^{(3)} = \cdots = f(\Delta X)$ and $\varphi_{13}^{(1)} = \varphi_{13}^{(2)} = \varphi_{13}^{(3)} = \cdots = g(\Delta X)$, where $\Delta X$ denotes a change in the driving conditions such as a variation, $\Delta\nu$, in the driving frequency or a change in the drivers' phase $\Delta\theta$. Here, we use upper scripts (1), (2) ... to label the phi-bits.

For the initialization, starting with the tensor product state, $\boldsymbol{V}$, we then define a new representation for the $N$ phi-bits such that the state at the crossing, $\Delta X^*$, can be described by $2^N \times 1$ vector containing all 1's and properly normalized by the factor $1/\sqrt{2^N}$. In the last step of the initialization, we find a unitary matrix, $\boldsymbol{U}_{2^N \times 2^N}$, which transforms the above vector into one with a 1 as the first component and all other $2^N - 1$ components become 0.

We then consider the general vector in this initialization representation by setting all $\varphi_{12}^{(i)}$'s to be $f$ and all $\varphi_{13}^{(i)}$'s to be $g$. Finally, we exchange $f$ and $g$, which is then to be described by a non-trivial transformation, $\boldsymbol{T}$, in the new representation.

We now illustrate initialization and transformation in the cases $N = 1$ through 5.

**Case I: $N = 1$.**

In this case, according to Eq. (2), we simply have $\boldsymbol{V}_{2\times 1} = \frac{1}{\sqrt{2}}\begin{pmatrix} \exp\left(i\varphi_{12}^{(1)}\right) \\ \exp\left(i\varphi_{13}^{(1)}\right) \end{pmatrix}$. Since $\varphi_{12}^{(1)}$ and $\varphi_{13}^{(1)}$ cross at $\Delta X^*$, at the crossing $\boldsymbol{V}_{2\times 1} = \frac{1}{\sqrt{2}}\begin{pmatrix} 1 \\ 1 \end{pmatrix}$ up to an overall phase that is neglected.

We need a unitary transformation $\boldsymbol{U}_{2\times 2}$ that zeros the second element. There are at least two possibilities, $\boldsymbol{U}_{2\times 2} = \frac{1}{\sqrt{2}}\begin{pmatrix} 1 & 1 \\ -1 & 1 \end{pmatrix}$ or $\boldsymbol{U}_{2\times 2} = \frac{1}{\sqrt{2}}\begin{pmatrix} 1 & 1 \\ 1 & -1 \end{pmatrix}$. Choosing the antisymmetric matrix $\boldsymbol{U}_{2\times 2}\boldsymbol{V}_{2\times 1} = \frac{1}{\sqrt{2}}\begin{pmatrix} 1 & 1 \\ -1 & 1 \end{pmatrix}\frac{1}{\sqrt{2}}\begin{pmatrix} 1 \\ 1 \end{pmatrix} = \begin{pmatrix} 1 \\ 0 \end{pmatrix}$. Note that this unitary transformation is skew-symmetric so that, in the parlance of quantum computing, it is irreversible, that is, applying it twice to a vector does not leave the vector unchanged. In our classical system, unitary matrices do not need to be reversible since the physical state of the system can be restored exactly as it was before after a transformation is performed.

The general vector in the transformed representation is, therefore,

$$\tilde{\boldsymbol{V}}_{2\times 1} = \boldsymbol{U}_{2\times 2}\boldsymbol{V}_{2\times 1} = \frac{1}{2}\begin{pmatrix} 1 & 1 \\ -1 & 1 \end{pmatrix}\begin{pmatrix} \exp\left(i\varphi_{12}^{(1)}\right) \\ \exp\left(i\varphi_{13}^{(1)}\right) \end{pmatrix}$$
$$= \frac{1}{2}\begin{pmatrix} \exp\left(i\varphi_{12}^{(1)}\right) + \exp\left(i\varphi_{13}^{(1)}\right) \\ -\exp\left(i\varphi_{12}^{(1)}\right) + \exp\left(i\varphi_{13}^{(1)}\right) \end{pmatrix}.$$

Setting $\varphi_{12}^{(1)} = f$ and $\varphi_{13}^{(1)} = g$ leads to

$$\tilde{\boldsymbol{V}}_{2\times 1} = \frac{1}{2}\begin{pmatrix} \exp(if) + \exp(ig) \\ -\exp(if) + \exp(ig) \end{pmatrix}.$$

Changing the drivers' physical parameters from $\Delta X_1$ to $\Delta X_2$ swaps the values of $f$ and $g$, yielding

$$\tilde{\boldsymbol{V}}'_{2\times 1} = \frac{1}{2}\begin{pmatrix} \exp(ig) + \exp(if) \\ -\exp(ig) + \exp(if) \end{pmatrix}.$$

We can find by inspection the transformation matrix $\boldsymbol{T}_{2\times2}$ for which $\boldsymbol{T}_{2\times2}\tilde{\boldsymbol{V}}_{2\times1} = \tilde{\boldsymbol{V}}'_{2\times1}$. This transformation matrix is given by

$$\boldsymbol{T}_{2\times2} = \begin{pmatrix} 1 & 0 \\ 0 & -1 \end{pmatrix}, \tag{4}$$

which is the Pauli spin matrix $\sigma_z$.

**Case II: $N = 2$.**

We define a two phi-bit representation as

$$\boldsymbol{V}_{4\times1} = \frac{1}{2}\begin{pmatrix} \exp(i\theta_1) \\ \exp(i\theta_2) \\ \exp(i\theta_3) \\ \exp(i\theta_4) \end{pmatrix},$$

where $\theta_1 = \varphi_{12}^{(1)} + \frac{1}{2}\varphi_{12}^{(2)}; \theta_2 = \varphi_{12}^{(1)} + \frac{1}{2}\varphi_{13}^{(2)}; \theta_3 = \varphi_{13}^{(1)} + \frac{1}{2}\varphi_{12}^{(2)}; \theta_4 = \varphi_{13}^{(1)} + \frac{1}{2}\varphi_{13}^{(2)}$.

Note the coefficient $1/2$ in the previous expression, which differentiates phi-bit 1 from phi-bit 2. At the crossing point $\Delta X^*$, neglecting an overall phase, this state vector becomes $\boldsymbol{V}_{4\times1} = \frac{1}{2}\begin{pmatrix} 1 \\ 1 \\ 1 \\ 1 \end{pmatrix}$.

Let us introduce the unitary matrix $\boldsymbol{U}_{4\times4} = \frac{1}{2}\begin{pmatrix} 1 & 1 & 1 & 1 \\ -\sqrt{2} & \sqrt{2} & 0 & 0 \\ 1 & 1 & -1 & -1 \\ 0 & 0 & -\sqrt{2} & \sqrt{2} \end{pmatrix}$ so that $\boldsymbol{U}_{4\times4}\boldsymbol{V}_{4\times1} = \begin{pmatrix} 1 \\ 0 \\ 0 \\ 0 \end{pmatrix}$. Applying this unitary matrix to the general state vector $\boldsymbol{V}_{4\times1}$ produces the new state vector $\tilde{\boldsymbol{V}}_{4\times1}$, which is given by

$$\tilde{\boldsymbol{V}}_{4\times1} = \frac{1}{4}\begin{pmatrix} \tilde{V}_1 \\ \tilde{V}_2 \\ \tilde{V}_3 \\ \tilde{V}_4 \end{pmatrix},$$

where $\tilde{V}_1 = \sum_{j=1}^{4} \exp(i\theta_j)$; $\tilde{V}_2 = -\sqrt{2}\exp(i\theta_1) + \sqrt{2}\exp(i\theta_2)$; $\tilde{V}_3 = \exp(i\theta_1) + \exp(i\theta_2) - \exp(i\theta_3) - \exp(i\theta_4)$; $\tilde{V}_4 = -\sqrt{2}\exp(i\theta_3) + \sqrt{2}\exp(i\theta_4)$.

Following our initialization process, we set $\varphi_{12}^{(1)} = \varphi_{12}^{(2)} = f$ and $\varphi_{13}^{(1)} = \varphi_{13}^{(2)} = g$, that is, $\theta_1 = \frac{3}{2}f; \theta_2 = f + \frac{1}{2}g; \theta_3 = \frac{1}{2}f + g; \theta_4 = \frac{3}{2}g$. To identify the transformation $\boldsymbol{T}_{4\times4}$, one swaps $f$ and $g$. The corresponding physical action of changing the physical parameter $\Delta X_1$ into $\Delta X_2$ exchanges the phases $\theta_1 \leftrightarrow \theta_4$ and $\theta_2 \leftrightarrow \theta_3$ so the state vector becomes $\tilde{\boldsymbol{V}}'_{4X1} = \frac{1}{4}\begin{pmatrix} \tilde{V}_1 \\ -\tilde{V}_4 \\ -\tilde{V}_3 \\ -\tilde{V}_2. \end{pmatrix}$.

The unitary transformation matrix that relates $\tilde{\boldsymbol{V}}'_{4\times1}$ to $\tilde{\boldsymbol{V}}_{4\times1}$ is easily found to be

$$\boldsymbol{T}_{4\times4} = \begin{pmatrix} 1 & 0 & 0 & 0 \\ 0 & 0 & 0 & -1 \\ 0 & 0 & -1 & 0 \\ 0 & -1 & 0 & 0 \end{pmatrix}. \tag{5}$$

This transformation keeps the first component of the state vector, changes the phase of the third component by π, and swaps the other two components plus a π phase change.

**Case III: $N = 3$.**

As vectors and matrices get larger, it is useful to make a few definitions. In what follows, all vectors will be composed of elements of the form $V_j = \exp(i\theta_j)$ so that specifying the $\theta_j$'s will define the vector. Furthermore, some $4 \times 4$ submatrices will help make large unitary transformation matrices more compact. For this, we define

$$\boldsymbol{A}(N) = \begin{pmatrix} 1 & 1 & 1 & 1 \\ -2^{\frac{N-1}{2}} & 2^{\frac{N-1}{2}} & 0 & 0 \\ 2^{\frac{N-2}{2}} & 2^{\frac{N-2}{2}} & -2^{\frac{N-2}{2}} & -2^{\frac{N-2}{2}} \\ 0 & 0 & -2^{\frac{N-1}{2}} & 2^{\frac{N-1}{2}} \end{pmatrix}$$

and

$$\boldsymbol{B} = \begin{pmatrix} 1 & 1 & 1 & 1 \\ 0 & 0 & 0 & 0 \\ 0 & 0 & 0 & 0 \\ 0 & 0 & 0 & 0 \end{pmatrix} = -\boldsymbol{C}.$$

For the $8 \times 1$ vector $\boldsymbol{V}_{8\times1}$, the elements include $\theta_1 = \varphi_{12}^{(1)} + \frac{2}{3}\varphi_{12}^{(2)} + \frac{1}{3}\varphi_{12}^{(3)}; \theta_2 = \varphi_{12}^{(1)} + \frac{2}{3}\varphi_{12}^{(2)} + \frac{1}{3}\varphi_{13}^{(3)}; \theta_3 = \varphi_{12}^{(1)} + \frac{2}{3}\varphi_{13}^{(2)} + \frac{1}{3}\varphi_{12}^{(3)}$; $\theta_4 = \varphi_{13}^{(1)} + \frac{2}{3}\varphi_{12}^{(2)} + \frac{1}{3}\varphi_{12}^{(3)}$; $\theta_5 = \varphi_{12}^{(1)} + \frac{2}{3}\varphi_{13}^{(2)} + \frac{1}{3}\varphi_{13}^{(3)}$; $\theta_6 = \varphi_{13}^{(1)} + \frac{2}{3}\varphi_{12}^{(2)} + \frac{1}{3}\varphi_{13}^{(3)}; \theta_7 = \varphi_{13}^{(1)} + \frac{2}{3}\varphi_{13}^{(2)} + \frac{1}{3}\varphi_{12}^{(3)}; \theta_8 = \varphi_{13}^{(1)} + \frac{2}{3}\varphi_{13}^{(2)} + \frac{1}{3}\varphi_{13}^{(3)}$.

At crossing, $f = g$, all elements are equal to 1 divided by the normalization factor $2\sqrt{2}$. Again, we have dropped a general phase. We now seek the unitary transformation $\boldsymbol{U}_{8\times8}$, which initializes the system at the crossing point, that is, it satisfies $\boldsymbol{U}_{8\times8}\boldsymbol{V}_{8\times1} = \begin{pmatrix} 1 \\ 0 \\ \cdot \\ 0 \end{pmatrix}$. This unitary matrix can be constructed as follows:

$$\boldsymbol{U}_{8\times8} = \frac{1}{2\sqrt{2}}\begin{pmatrix} \boldsymbol{A}(3) & \boldsymbol{B} \\ \boldsymbol{C} & \boldsymbol{A}(3) \end{pmatrix}.$$

Applying this unitary matrix to the general three phi-bit state vector leads to the vector in the new basis $\tilde{\boldsymbol{V}}$, whose elements are given by

$\tilde{V}_1 = \sum_{j=1}^{8} \exp(i\theta_j)$; $\tilde{V}_2 = -2\exp(i\theta_1) + 2\exp(i\theta_2)$; $\tilde{V}_3 = \sqrt{2}\exp(i\theta_1) + \sqrt{2}\exp(i\theta_2) - \sqrt{2}\exp(i\theta_3) - \sqrt{2}\exp(i\theta_4)$; $\tilde{V}_4 = -2\exp(i\theta_3) + 2\exp(i\theta_4)$; $\tilde{V}_5 = \sum_{j=1}^{4}\exp(i\theta_j) - \sum_{j=5}^{8}\exp(i\theta_j)$; $\tilde{V}_6 = -2\exp(i\theta_5) + 2\exp(i\theta_6)$; $\tilde{V}_7 = \sqrt{2}\exp(i\theta_5) + \sqrt{2}\exp(i\theta_6) - \sqrt{2}\exp(i\theta_7) - \sqrt{2}\exp(i\theta_8)$; $\tilde{V}_8 = -2\exp(i\theta_7) + 2\exp(i\theta_8)$.

By setting $\varphi_{12}^{(1)} = \varphi_{12}^{(2)} = \varphi_{12}^{(3)} = f$ and $\varphi_{13}^{(1)} = \varphi_{13}^{2} = \varphi_{13}^{(3)} = g$, we have $\theta_1 = 2f; \theta_2 = \frac{5}{3}f + \frac{1}{3}g; \theta_3 = \frac{4}{3}f + \frac{2}{3}g; \theta_4 = f + g; \theta_5 = f + g; \theta_6 = \frac{2}{3}f + \frac{4}{3}g; \theta_7 = \frac{1}{3}f + \frac{5}{3}g; \theta_8 = 2g$.

Through physical action on the drivers' parameters, $\Delta X_1 \to \Delta X_2$, one swaps $f$ and $g$. This action exchanges the phases $\theta_1 \leftrightarrow \theta_8$; $\theta_2 \leftrightarrow \theta_7$; $\theta_3 \leftrightarrow \theta_6$; $\theta_4 \leftrightarrow \theta_5$. These phase swaps lead to the new vector in the chosen representation, $\tilde{\boldsymbol{V}}'_{8\times1}$, with elements $\tilde{V}'_1 = \tilde{V}_1; \tilde{V}'_2 = -\tilde{V}_8; \tilde{V}'_3 = -\tilde{V}_7; \tilde{V}'_4 = -\tilde{V}_6; \tilde{V}'_5 = -\tilde{V}_5; \tilde{V}'_6 = -\tilde{V}_4; \tilde{V}'_7 = -\tilde{V}_3; \tilde{V}'_8 = -\tilde{V}_2$. This new vector is related to $\boldsymbol{V}_{8\times1}$ by the transformation $\tilde{\boldsymbol{V}}'_{8\times1} = \boldsymbol{T}_{8\times8}\boldsymbol{V}_{8\times1}$. The transformation matrix can be constructed by inspections as

$$\boldsymbol{T}_{8\times8} = \begin{pmatrix} \boldsymbol{T}_p & \boldsymbol{T}_a \\ \boldsymbol{T}_a & -\boldsymbol{T}_p \end{pmatrix}, \tag{6}$$

where we introduce the $4\times4$ submatrices

$$\boldsymbol{T}_p = \begin{pmatrix} 1 & 0 & 0 & 0 \\ 0 & 0 & 0 & 0 \\ 0 & 0 & 0 & 0 \\ 0 & 0 & 0 & 0 \end{pmatrix} \quad \text{and} \quad \boldsymbol{T}_a = \begin{pmatrix} 0 & 0 & 0 & 0 \\ 0 & 0 & 0 & -1 \\ 0 & 0 & -1 & 0 \\ 0 & -1 & 0 & 0 \end{pmatrix}.$$

These submatrices will be employed when addressing the scalability of initialization and the transformation, $\boldsymbol{T}$, beyond three phi-bits.

**Case IV: $N = 4$.**

The four phi-bit state vector $\boldsymbol{V}_{16\times1}$ is normalized by $\frac{1}{4}$ and is composed of the elements $V_j = \exp(i\theta_j)$, with $\theta_1 = \varphi_{12}^{(1)} + \frac{3}{4}\varphi_{12}^{(2)} + \frac{1}{2}\varphi_{12}^{(3)} + +\frac{1}{4}\varphi_{12}^{(4)}; \theta_2 = \varphi_{12}^{(1)} + \frac{3}{4}\varphi_{12}^{(2)} + \frac{1}{2}\varphi_{12}^{(3)} + \frac{1}{4}\varphi_{13}^{(4)}; \theta_3 = \varphi_{12}^{(1)} + \frac{3}{4}\varphi_{12}^{(2)} + \frac{1}{2}\varphi_{13}^{(3)} + \frac{1}{4}\varphi_{12}^{(4)}; \theta_4 = \varphi_{12}^{(1)} + \frac{3}{4}\varphi_{13}^{(2)} + \frac{1}{2}\varphi_{12}^{(3)} + \frac{1}{4}\varphi_{12}^{(4)}; \theta_5 = \varphi_{13}^{(1)} + \frac{3}{4}\varphi_{12}^{(2)} + \frac{1}{2}\varphi_{12}^{(3)} + \frac{1}{4}\varphi_{12}^{(4)}; \theta_6 = \varphi_{12}^{(1)} + \frac{3}{4}\varphi_{12}^{(2)} + \frac{1}{2}\varphi_{13}^{(3)} + \frac{1}{4}\varphi_{13}^{(4)}; \theta_7 = \varphi_{12}^{(1)} + \frac{3}{4}\varphi_{13}^{(2)} + \frac{1}{2}\varphi_{12}^{(3)} + \frac{1}{4}\varphi_{13}^{(4)}; \theta_8 = \varphi_{13}^{(1)} + \frac{3}{4}\varphi_{12}^{(2)} + \frac{1}{2}\varphi_{12}^{(3)} + \frac{1}{4}\varphi_{13}^{(4)}; \theta_9 = \varphi_{12}^{(1)} + \frac{3}{4}\varphi_{13}^{(2)} + \frac{1}{2}\varphi_{13}^{(3)} + \frac{1}{4}\varphi_{12}^{(4)}; \theta_{10} = \varphi_{13}^{(1)} + \frac{3}{4}\varphi_{12}^{(2)} + \frac{1}{2}\varphi_{13}^{(3)} + \frac{1}{4}\varphi_{12}^{(4)}; \theta_{11} = \varphi_{13}^{(1)} + \frac{3}{4}\varphi_{13}^{(2)} + \frac{1}{2}\varphi_{12}^{(3)} + \frac{1}{4}\varphi_{12}^{(4)}; \theta_{12} = \varphi_{12}^{(1)} + \frac{3}{4}\varphi_{13}^{(2)} + \frac{1}{2}\varphi_{13}^{(3)} + \frac{1}{4}\varphi_{13}^{(4)}; \theta_{13} = \varphi_{13}^{(1)} + \frac{3}{4}\varphi_{12}^{(2)} + \frac{1}{2}\varphi_{13}^{(3)} + \frac{1}{4}\varphi_{13}^{(4)}; \theta_{14} = \varphi_{13}^{(1)} + \frac{3}{4}\varphi_{13}^{(2)} + \frac{1}{2}\varphi_{12}^{(3)} + \frac{1}{4}\varphi_{13}^{(4)}; \theta_{15} = \varphi_{13}^{(1)} + \frac{3}{4}\varphi_{13}^{(2)} + \frac{1}{2}\varphi_{13}^{(3)} + \frac{1}{4}\varphi_{12}^{(4)}; \theta_{16} = \varphi_{13}^{(1)} + \frac{3}{4}\varphi_{13}^{(2)} + \frac{1}{2}\varphi_{13}^{(3)} + \frac{1}{4}\varphi_{13}^{(4)}$.

The unitary transformation $\boldsymbol{U}_{16\times16}$ is expressed in terms of $4\times4$ submatrices $\boldsymbol{A}(N = 4)$, $\boldsymbol{B}$, and $\boldsymbol{C}$. There are a number of options for the unitary transformations that accomplish our aim of finding a representation for $\tilde{\boldsymbol{V}}_{16\times1}$. Recalling that the unitary transformation for $N = 3$ is $\boldsymbol{U}_{8\times8} = \frac{1}{2\sqrt{2}}\begin{pmatrix} \boldsymbol{A}(3) & \boldsymbol{B} \\ \boldsymbol{C} & \boldsymbol{A}(3) \end{pmatrix}$, we construct $\boldsymbol{U}_{16\times16}$ by using $\boldsymbol{U}_{8\times8}$ as a submatrix along the diagonal. For instance,

$$\boldsymbol{U}_{16\times16} = \frac{1}{2}\begin{pmatrix} \boldsymbol{A}(4) & \boldsymbol{B} & \boldsymbol{B} & \boldsymbol{B} \\ \boldsymbol{C} & \boldsymbol{A}(4) & \boldsymbol{B} & \boldsymbol{C} \\ \boldsymbol{C} & \boldsymbol{C} & \boldsymbol{A}(4) & \boldsymbol{B} \\ \boldsymbol{C} & \boldsymbol{B} & \boldsymbol{C} & \boldsymbol{A}(4) \end{pmatrix}.$$

Looking at the unitary transformations $\boldsymbol{U}$ for $N = 3$ and $N = 4$, we can see that the diagonal contains the unitary transformation for the previous $N$ with $\boldsymbol{A}$ updated to the $N$ under consideration [e.g., $\boldsymbol{A}(3) \to \boldsymbol{A}(4)$ as $N = 3 \to N = 4$]. Noting that the first row of $\boldsymbol{A}$ and $\boldsymbol{B}$ is composed of +1's and that of $\boldsymbol{C}$ is composed of −1's. Referring to the first two $4\times4$ submatrices as images and to $\boldsymbol{C}$ as an anti-image, we can think of the upper (lower) off-diagonal submatrix in $\boldsymbol{U}_{8\times8}$ as being symmetric (antisymmetric). Following that theme, we see that the $\boldsymbol{U}_{16\times16}$ can be constructed by taking the symmetric image of $\boldsymbol{U}_{8\times8}$ in the upper off-diagonal block and mirroring it. Similarly, the lower off-diagonal block can be obtained by mirroring the antisymmetric image of $\boldsymbol{U}_{8\times8}$.

Applying this unitary matrix to the general three phi-bit state vector leads to the vector in the new basis $\tilde{\boldsymbol{V}}_{16\times1}$. With the physical action swapping $f$ and $g$, to create the state vector $\tilde{\boldsymbol{V}}'_{16\times1}$, we obtain the following transformation matrix:

$$\boldsymbol{T}_{16\times16} = \begin{pmatrix} \boldsymbol{T}_p & 0 & 0 & \boldsymbol{T}_a \\ 0 & \boldsymbol{T}_p & \boldsymbol{T}_a & 0 \\ 0 & \boldsymbol{T}_a & -\boldsymbol{T}_p & 0 \\ \boldsymbol{T}_a & 0 & 0 & -\boldsymbol{T}_p \end{pmatrix}. \tag{7}$$

**Case V: $N = 5$.**

The prescription for forming the unitary transformation $\boldsymbol{U}$ for $N+1$, which is rank $2^{N+1}$, is to form 4 rank $2^N$ submatrices. The diagonal submatrices are the unitary transformations from $N$ with $\boldsymbol{A}(N)$ replaced by $\boldsymbol{A}(N+1)$ and the off-diagonal submatrices formed from the symmetric and antisymmetric mirrored images of the unitary transformation from $N$. For the case of $N = 5$, we need a more compact notation since the matrix is now $32\times32$. The 32 phases $(\theta_1, \ldots, \theta_{32})$ are defined by linear combinations of $\varphi_{12}$ and $\varphi_{13}$ with coefficients 1, 4/5, 3/5, 2/5, 1/5, such as $\theta_1 = \varphi_{12}^{(1)} + \frac{4}{5}\varphi_{12}^{(2)} + \frac{3}{5}\varphi_{12}^{(3)} + \frac{2}{5}\varphi_{12}^{(4)} + \frac{1}{5}\varphi_{12}^{(5)}$, and permutations for the five phi-bit upper scripts. We also note that $\theta_i \leftrightarrow \theta_j$ for all $i + j = 33$. The initial $32\times1$ vector at the crossing point contains all 1's up to an overall phase and normalization constant $\frac{1}{4\sqrt{2}}$. Now, we write the unitary transformation that takes the initial $32\times1$ vector into a vector with a 1 for the first component and 0 for all other components,

$$\boldsymbol{U}_{32\times32} = \frac{1}{4\sqrt{2}}\begin{pmatrix} \boldsymbol{U}_{16\times16}(5) & \boldsymbol{M}^{S}_{16\times16} \\ \boldsymbol{M}^{A}_{16\times16} & \boldsymbol{U}_{16\times16}(5) \end{pmatrix},$$

where $\boldsymbol{U}_{16\times16}(5)$ is the form of the $16\times16$ unitary transformation without the normalization factor $\frac{1}{2}$, and $\boldsymbol{A}(4)$ replaced by $\boldsymbol{A}(5)$. The matrix $\boldsymbol{M}^{S}_{16\times16}$ ($\boldsymbol{M}^{A}_{16\times16}$) is the symmetric (antisymmetric) mirrored image of $\boldsymbol{U}_{16\times16}$,

$$\boldsymbol{M}^{S}_{16\times16} = \begin{pmatrix} \boldsymbol{B} & \boldsymbol{B} & \boldsymbol{B} & \boldsymbol{B} \\ \boldsymbol{C} & \boldsymbol{B} & \boldsymbol{B} & \boldsymbol{C} \\ \boldsymbol{B} & \boldsymbol{B} & \boldsymbol{C} & \boldsymbol{C} \\ \boldsymbol{B} & \boldsymbol{C} & \boldsymbol{B} & \boldsymbol{C} \end{pmatrix},$$

and

$$\boldsymbol{M}^{A}_{16\times16} = \begin{pmatrix} \boldsymbol{C} & \boldsymbol{C} & \boldsymbol{C} & \boldsymbol{C} \\ \boldsymbol{B} & \boldsymbol{C} & \boldsymbol{C} & \boldsymbol{B} \\ \boldsymbol{C} & \boldsymbol{C} & \boldsymbol{B} & \boldsymbol{B} \\ \boldsymbol{C} & \boldsymbol{B} & \boldsymbol{C} & \boldsymbol{B} \end{pmatrix}.$$

It is straightforward to check that $\boldsymbol{U}_{32\times32}$ is unitary by calculating

$$\boldsymbol{U}_{32\times32}\boldsymbol{U}^{T}_{32\times32} = \frac{1}{32}\begin{pmatrix} \boldsymbol{U}_{16\times16}(5)\boldsymbol{U}^{T}_{16\times16}(5) + \boldsymbol{M}^{S}_{16\times16}\left(\boldsymbol{M}^{S}_{16\times16}\right)^{T} & \boldsymbol{U}_{16\times16}(5)\left(\boldsymbol{M}^{A}_{16\times16}\right)^{T} + \boldsymbol{M}^{S}_{16\times16}\boldsymbol{U}^{T}_{16\times16}(5) \\ \boldsymbol{M}^{A}_{16\times16}\boldsymbol{U}^{T}_{16\times16}(5) + \boldsymbol{U}_{16\times16}(5)\left(\boldsymbol{M}^{S}_{16\times16}\right)^{T} & \boldsymbol{U}_{16\times16}(5)\boldsymbol{U}^{T}_{16\times16}(5) + \boldsymbol{M}^{A}_{16\times16}\left(\boldsymbol{M}^{A}_{16\times16}\right)^{T} \end{pmatrix},$$

$\boldsymbol{U}_{32\times32}\boldsymbol{U}^{T}_{32\times32} = \boldsymbol{I}_{32\times32}$. Following our procedure, by applying this unitary transformation onto the general vector $\boldsymbol{V}_{32\times1}$, to obtain the vector $\tilde{\boldsymbol{V}}_{32\times1}$ and swapping $f$ and $g$, yields $\tilde{\boldsymbol{V}}'_{32\times1}$. This later vector is related to $\tilde{\boldsymbol{V}}_{32\times1}$ by the following transformation matrix:

$$\boldsymbol{T} = \begin{pmatrix} \boldsymbol{T}_p & 0 & 0 & 0 & 0 & 0 & 0 & \boldsymbol{T}_a \\ 0 & \boldsymbol{T}_p & 0 & 0 & 0 & 0 & \boldsymbol{T}_a & 0 \\ 0 & 0 & \boldsymbol{T}_p & 0 & 0 & \boldsymbol{T}_a & 0 & 0 \\ 0 & 0 & 0 & \boldsymbol{T}_p & \boldsymbol{T}_a & 0 & 0 & 0 \\ 0 & 0 & 0 & \boldsymbol{T}_a & -\boldsymbol{T}_p & 0 & 0 & 0 \\ 0 & 0 & \boldsymbol{T}_a & 0 & 0 & -\boldsymbol{T}_p & 0 & 0 \\ 0 & \boldsymbol{T}_a & 0 & 0 & 0 & 0 & -\boldsymbol{T}_p & 0 \\ \boldsymbol{T}_a & 0 & 0 & 0 & 0 & 0 & 0 & -\boldsymbol{T}_p \end{pmatrix}. \quad (8)$$

**Case VI: From $N$ to $N$+1.**

One can use the result for five logical phi-bits to determine the initial state vector and corresponding transformation matrix for six logical phi-bits. The series of transformation matrices given by Eqs. (4)–(8) for $N = 1, 2, 3, 4$, and 5 logical phi-bits form the foundation for proving by induction that the process of initialization and transformation generalizes from any $N$ phi-bits to $N+1$ phi-bits. This inductive procedure presented below demonstrates the scalability of multiple phi-bit vector states and the non-trivial transformation associated with an action on the phi-bit supporting acoustic metamaterial.

We assume that the unitary transformation exists for $N$ and show that the above procedure creates the unitary transformation for $N+1$. To simplify the notation, we define $d = 2^N$ and $d' = 2^{N+1}$. We posit that

$$\boldsymbol{U}_{d'\times d'} = \frac{1}{\sqrt{d'}}\begin{pmatrix} \boldsymbol{U}_{d\times d}(N+1) & \boldsymbol{M}^{S}_{d\times d} \\ -\boldsymbol{M}^{S}_{d\times d} & \boldsymbol{U}_{d\times d}(N+1) \end{pmatrix}. \quad (9)$$

First, we have verified that this is a unitary transformation by taking the product of the matrix with its transform (see the Appendix).

The form of the transformation matrix on the exchange of $f$ and $g$ can be described by two $d\times d$ dimensional matrices: a diagonal matrix, $\boldsymbol{T}^{p}_{d\times d}$, composed of blocks of the $\boldsymbol{T}_p$ $4\times4$ matrix, and an antidiagonal matrix, $\boldsymbol{T}^{a}_{d\times d}$, composed of blocks of the $\boldsymbol{T}_a 4\times4$ matrix as

$$\boldsymbol{T}_{d'\times d'} = \begin{pmatrix} \boldsymbol{T}^{p}_{d\times d} & \boldsymbol{T}^{a}_{d\times d} \\ \boldsymbol{T}^{a}_{d\times d} & -\boldsymbol{T}^{p}_{d\times d} \end{pmatrix}. \quad (10)$$

The generalized form of the unitary transformation defining the representation in the $2^{N+1}$ space and the transformation in that representation complete the demonstration that the above procedure scales to all $N$, i.e., the procedure is robustly scalable.

## IV. CONCLUSIONS

We have established a correspondence between the state of logical phi-bits, classical nonlinear acoustic analog of qubits, represented in a low-dimensional linearly scaling physical space of an externally driven acoustic metamaterial and a multiple phi-bit state representation as a complex vector in a high-dimensional, exponentially scaling Hilbert space. We used an inductive procedure to demonstrate the scalability of the initialization and the unitary transformations of exponentially complex superpositions of states of multiple correlated logical phi-bits. We also show that manipulating the phi-bits in the physical space enables the implementation of a non-trivial multiple phi-bit unitary transformation. This scalable transformation operates in parallel on the components of the multiple phi-bit complex state vector, requiring only a single physical action on the metamaterial. This work shows that we can realize large-scale multiple phi-bit unitary operations on nonlinear acoustic metamaterials and transformations that do not require decomposition into quantum-like circuits of single- and two-qubit gates. This study is one significant step in demonstrating that logical phi-bits present advantageous scalable algorithm development approaches that are unaffected by measurements and decoherence. This advantage makes nonlinear externally driven acoustic metamaterials a potentially compelling option to complement existing quantum computing technologies.

## ACKNOWLEDGMENTS

The development of the apparatus was supported in part by a grant from the W.M. Keck foundation. P.A.D. and J.A.L. acknowledge the partial support from NSF Grant No. 2204400. M.A.H. acknowledges the partial support from NSF Grant No. 2204382 and acknowledges Wayne State University Startup funds for additional support. This work was also partially supported by the Science and Technology Center New Frontiers of Sound (NewFoS) through NSF Grant No. 2242925.

## AUTHOR DECLARATIONS

### Conflict of Interest

The authors have no conflicts to disclose.

### Author Contributions

**K. Runge**: Conceptualization (equal); Formal analysis (equal); Funding acquisition (equal); Investigation (equal); Methodology (equal); Validation (equal); Writing – original draft (equal). **P. A. Deymier**: Conceptualization (equal); Formal analysis (equal); Funding acquisition (equal); Investigation (equal); Methodology (equal); Validation (equal); Writing – review & editing (equal). **M. A. Hasan**: Conceptualization (equal); Formal analysis (equal); Funding acquisition (equal); Investigation (equal); Methodology (equal); Writing – review & editing (equal). **T. D. Lata**: Conceptualization (equal); Investigation (equal); Methodology (equal); Validation (equal); Writing – review & editing (equal). **J. A. Levine**: Conceptualization (equal); Funding acquisition (equal); Investigation (equal); Methodology (equal); Validation (equal); Writing – review & editing (equal).

## DATA AVAILABILITY

The data that support the findings of this study are available within the article.

## APPENDIX: UNITARITY DEMONSTRATION FOR N PHI-BIT TRANSFORMATION

$$\boldsymbol{U}_{d'\times d'}\boldsymbol{U}^T_{d'\times d'} = \frac{1}{d'}\begin{pmatrix} \boldsymbol{U}_{d\times d}(N+1)\boldsymbol{U}^T_{d\times d}(N+1) + \boldsymbol{M}^{\boldsymbol{S}}_{d\times d}\left(\boldsymbol{M}^{\boldsymbol{S}}_{d\times d}\right)^T & -\boldsymbol{U}_{d\times d}(N+1)\left(\boldsymbol{M}^{\boldsymbol{S}}_{d\times d}\right)^T + \boldsymbol{M}^{\boldsymbol{S}}_{d\times d}\boldsymbol{U}^T_{d\times d}(N+1) \\ -\boldsymbol{M}^{\boldsymbol{S}}_{d\times d}\boldsymbol{U}^T_{d\times d}(N+1) + \boldsymbol{U}_{d\times d}(N+1)\left(\boldsymbol{M}^{\boldsymbol{S}}_{dXd}\right)^T & \boldsymbol{U}_{d\times d}(N+1)\boldsymbol{U}^T_{d\times d}(N+1) + \boldsymbol{M}^{\boldsymbol{S}}_{d\times d}\left(\boldsymbol{M}^{\boldsymbol{S}}_{d\times d}\right)^T \end{pmatrix}.$$

Let us begin by considering that the off-diagonal blocks $\boldsymbol{U}_{d\times d}$ are composed of the $4\times 4$ submatrices $\boldsymbol{A}(N)$, $\boldsymbol{B}$, and $\boldsymbol{C}$, and the off-diagonal blocks are comprised of matrix products of these submatrices. Note that the product

$$\boldsymbol{A}(N+1)\boldsymbol{B}^T = \begin{pmatrix} 4 & 0 & 0 & 0 \\ 0 & 0 & 0 & 0 \\ 0 & 0 & 0 & 0 \\ 0 & 0 & 0 & 0 \end{pmatrix} = \boldsymbol{B}\boldsymbol{A}^T(N+1) = \boldsymbol{B}\boldsymbol{B}^T = \boldsymbol{C}\boldsymbol{C}^T$$
$$= -\boldsymbol{A}(N+1)\boldsymbol{C}^T = -\boldsymbol{C}\boldsymbol{A}^T(N+1) = -\boldsymbol{B}\boldsymbol{C}^T = -\boldsymbol{C}\boldsymbol{B}^T.$$

The elements of off-diagonal blocks can be written as summations over the $4\times 4$ submatrices as follows:

$$\left[-\boldsymbol{U}_{d\times d}(N+1)\left(\boldsymbol{M}^{\boldsymbol{S}}_{d\times d}\right)^T + \boldsymbol{M}^{\boldsymbol{S}}_{d\times d}\boldsymbol{U}^T_{d\times d}(N+1)\right]_{ik}$$
$$= \sum_{j=1}^{d/4}\left(-U_{ij}\left(M^S_{jk}\right)^T + M^S_{ij}U^T_{jk}\right).$$

Recalling how the symmetric mirrored image is constructed and the product relations above, we can write, by letting $\frac{d}{4} = l$,

$$\sum_{j=1}^{l}\left(-U_{ij}\left(M^S_{jk}\right)^T + M^S_{ij}U^T_{jk}\right)$$
$$= \sum_{j=1}^{l}\left(-M^S_{i(l-j+1)}{M^S_{kj}}^T + M^S_{ij}M^S_{k(l-j+1)}\right),$$

and by letting $j' = l - j + 1$ in the second summation, we see that

$$\sum_{j=1}^{l}\left(-U_{ij}\left(M^S_{jk}\right)^T + M^S_{ij}U^T_{jk}\right) = \sum_{j=1}^{l} -M^S_{i(l-j+1)}{M^S_{kj}}^T$$
$$+ \sum_{j'=1}^{l} M^S_{i(l-j'+1)}M^S_{kj'},$$

which cancels term by term such that the off-diagonal blocks are the $d\times d$ null matrix.

In considering the diagonal blocks, recall the definition of $\boldsymbol{A}(N)$,

$$A(N) = \begin{pmatrix} 1 & 1 & 1 & 1 \\ -2^{\frac{N-1}{2}} & 2^{\frac{N-1}{2}} & 0 & 0 \\ 2^{\frac{N-2}{2}} & 2^{\frac{N-2}{2}} & -2^{\frac{N-2}{2}} & -2^{\frac{N-2}{2}} \\ 0 & 0 & -2^{\frac{N-1}{2}} & 2^{\frac{N-1}{2}} \end{pmatrix},$$

which is on the diagonal of $U_{d\times d}(N+1)$ forming the first product in the diagonal block of $U_{d'\times d'}U^T_{d'\times d'}$. We need to evaluate

$$A(N+1)A^T(N+1) = \begin{pmatrix} 4 & 0 & 0 & 0 \\ 0 & 2^{N+1} & 0 & 0 \\ 0 & 0 & 2^{N+1} & 0 \\ 0 & 0 & 0 & 2^{N+1} \end{pmatrix},$$

which appears $2^{N-1}$ times on the diagonal. As noted above, both $BB^T$ and $CC^T$ add 4 to the (1,1) element of this matrix. Furthermore, $U_{d\times d}$ is a unitary matrix so that its off-diagonal blocks are null matrices. Finally, $M^S_{d\times d}(M^S_{d\times d})^T$ contains $BB^T$ and $CC^T$ on its diagonal, and null matrix off-diagonal blocks so that the diagonal elements of the $U_{d'\times d'}$ are $d'$ and all other elements are zero, including the normalization constant, $\frac{1}{d'}$, and we see that $U_{d'\times d'}$ is unitary.

## REFERENCES


1. L. Calderin, M. A. Hasan, N. Jenkins, T. Lata, P. Lucas, K. Runge, and P. A. Deymier, Sci. Rep. **9**, 14156 (2019).
2. M. A. Hasan, L. Calderin, T. Lata, P. Lucas, K. Runge, and P. A. Deymier, Commun. Phys. **2**, 106 (2019).
3. M. A. Hasan, L. Calderín, T. Lata, P. Lucas, K. Runge, and P. A. Deymier, Appl. Phys. Lett. **116**, 164104 (2020).
4. M. A. Hasan, K. Runge, and P. A. Deymier, Sci. Rep. **11**, 24248 (2021).
5. P. A. Deymier, K. Runge, M. A. Hasan, T. D. Lata, J. A. Levine, and P. Cutillas, Sci. Rep. **13**, 635 (2023).
6. P. A. Deymier, K. Runge, M. A. Hasan, J. A. Levine, and P. Cutillas, Modell. Simul. Mater. Sci. Eng. **30**, 084003 (2022).
7. K. Runge, M. A. Hasan, J. A. Levine, and P. A. Deymier, Sci. Rep. **12**, 14066 (2022).
8. P. A. Deymier, K. Runge, P. Cutillas, M. A. Hasan, T. D. Lata, and J. A. Levine, Appl. Phys. Lett. **122**, 141701 (2023).
9. P. A. Deymier, K. Runge, M. A. Hasan, T. D. Lata, and J. A. Levine, Quantum Rep. **5**, 325 (2023).
10. P. DiVincenzo, Fortschr. Phys. **48**, 771 (2000).
11. L. Calderin, M. A. Hasan, K. Runge, and P. A. Deymier, J. Appl. Phys. **128**, 045110 (2020).
12. M. A. Hasan, L. Calderin, T. Lata, P. Lucas, K. Runge, and P. A. Deymier, Appl. Sci. **10**, 3202 (2020).
13. P. A. Deymier, K. Runge, and M. A. Hasan, Wave Motion **113**, 102977 (2022).
14. P. A. Deymier, M. A. Hasan, and K. Runge, AIP Adv. **10**, 095101 (2020).
15. P. A. Deymier and K. Runge, AIP Adv. **7**, 045020 (2017).
16. P. A. Deymier, K. Runge, M. A. Hasan, and L. Calderin, Materials **12**, 3553 (2019).
17. P. A. Deymier, K. Runge, and M. A. Hasan, J. Phys. Commun. **4**, 085018 (2020).
18. P. B. M. Sousa and R. V. Ramos, Quantum Inf. Comput. **7**, 228 (2007).
19. A. Barenco, C. H. Bennett, R. Cleve, D. P. DiVincenzo, N. Margolus, P. Shor, T. Sleator, J. A. Smolin, and H. Weinfurter, Phys. Rev. A **52**, 3457 (1995).
20. M. A. Nielsen and I. L. Chuang, Phys. Rev. Lett. **79**, 321 (1997).
21. B. Lanyon, M. Barbieri, M. Almeida *et al.*, Nat. Phys. **5**, 134 (2009).
22. A. Daskin, A. Grama, G. Kollias, and S. Kais, J. Chem. Phys. **137**, 234112 (2012).
23. D. Bera, S. Fenner, F. Green, and S. Homer, "Efficient universal quantum circuits," in *Computing and Combinatorics. COCOON 2009*, *Lecture Notes in Computer Science*, edited by H. Q. Ngo (Springer, Berlin, Heidelberg, 2009), Vol. 5609.
24. M. Frimmer and L. Novotny, Am. J. Phys. **82**, 947 (2014).